Kim *et al. EURASIP Journal on Wireless Communications and Networking* (2017) 2017:17
DOI 10.1186/s13638-016-0756-4

EURASIP Journal on Wireless Communications and Networking

RESEARCH **Open Access**

Low-complexity lattice reduction algorithm for MIMO detectors with tree searching

Hyunsub Kim, Hyukyeon Lee, Jihye Koo and Jaeseok Kim*

Abstract

In this paper, we propose a low-complexity lattice reduction (LR) algorithm for multiple-input multiple-output (MIMO) detectors with tree searching. Whereas conventional approaches are based exclusively on channel characteristics, we focus on joint optimisation by employing an early termination criterion in the context of MIMO detection. In this regard, incremental LR (ILR) was previously proposed. However, the ILR is limited to LR-aided successive interference cancellation (SIC) detectors which have considerable bit-error-rate (BER) performance degradation compared to optimal detectors. Hence, in this paper, we extend the conventional ILR to be applicable to the LR-aided detectors with near-optimal performance. Furthermore, we perform the hypothetical analysis and several novel modifications to handle the obstacles for the application of the ILR to LR-aided detectors other than the LR-aided SIC detectors. The simulation results demonstrate that the computational complexity is considerably reduced, with BER performance degradation of 10^{-5}.

Keywords: Lattice reduction, Multiple-input multiple-output, Early termination, Incremental lattice reduction

1 Introduction

In an effort to satisfy the demand for high-capacity wireless communication systems, ample research is currently dedicated to multiple-input multiple-output (MIMO) techniques, owing to their ability to provide diversity and multiplexing gain within limited bandwidth and power resources. However, a major obstacle to the realization of an enhanced MIMO system is the high computational complexity of its receiver. The optimal MIMO receiver is the maximum-likelihood (ML) detector (MLD). However, its complexity increases exponentially with the number of transmit antennas, making it infeasible for actual systems. Hence, a low-complexity design for MIMO receivers is a challenging research topic.

The sphere detector (SD) was introduced to achieve an optimal performance with low complexity, by employing a tree-searching algorithm [1, 2]. However, the variable complexity of the SD is a major drawback for practical systems that require data to be processed at a constant rate. To overcome this drawback, the fixed-complexity SD (FSD) [3, 4] and the K-best detector [5] have been developed. These detectors have the advantage of constant throughput, because there is no feedback in the data flow. In particular, the FSD approaches optimal performance in a fixed number of operations. Nevertheless, the complexity of these algorithms remains high in MIMO systems with a large number of transmit antennas and higher order modulation.

Recently, lattice reduction (LR)-aided detection methods have emerged as an efficient solution to the MIMO symbol-detection problem [6]. LR-aided linear and successive interference cancellation (SIC) detectors [7] provide the same diversity order as the ML detector, by transforming the system model with near-orthogonal channel matrices [8, 9]. Furthermore, the LR-aided K-best detector employs the Schnorr–Euchner enumeration to find the next child during tree searching [10–12]. However, a considerable gap remains between the performance of the optimal detector and those of conventional LR-aided detectors as the number of transmit antennas increases. In this regard, an LR-aided FSD has been developed to achieve near-ML performance,

*Correspondence: jaekim@yonsei.ac.kr
Department of Electrical and Electronic Engineering, Yonsei University, Shinchon-dong, Seodaemun-gu, 120-749 Seoul, Republic of Korea

despite a large number of antennas and higher order modulation [13–15].

Given these desirable features, research into LR-aided detection has remained active. The majority of research on LR-aided detection has been directed at a low-complexity LR algorithm. In [16], the complex-valued extension of the Lenstra–Lenstra–Lovász (LLL) [17] algorithm was proposed to reduce by half the size of the real-valued channel matrix. In [18], an effective LLL was proposed to reduce the complexity of the size reduction by processing only pairs of consecutive basis vectors. Moreover, some researchers focused on relaxing the Lovász condition to reduce complexity [19, 20]. Some effort in this field is devoted to fixing the complexity of the LLL algorithm. After the fixed-complexity LLL (fcLLL) algorithm was first proposed in [21], its complexity was further reduced by modifying the column traverse strategy [22–24].

Whereas these approaches focus exclusively on channel characteristics, another approach is to jointly optimise LR processing and the detection process. The approach is referred to as incremental LR (ILR) [25]. ILR performs partial SIC detection at each iteration and employs an early termination (ET) criterion based on the reliability assessment (RA) [26] computed with the partial detection result. However, ILR cannot be applied to LR-aided detectors other than the LR-aided SIC detector.

In this paper, we propose a low-complexity LR algorithm with ET that can be employed to high-performance LR-aided FSDs. In order to obtain the partial detection result in a simple manner, the proposed algorithm modifies the index of the column vectors for the channel matrix. Furthermore, in order to ensure that the characteristics of the lattice-reduced channel matrix remain the same, LR processing is performed only on the column vectors that involve LR-aided detection, and a modified QR decomposition (QRD) is proposed to generate the partially upper triangular matrix. The experimental results demonstrate that the proposed method achieves a significant reduction in complexity while maintaining a performance degradation of less than 0.5 dB at a bit error rate (BER) of 10^{-5} for a 8×8 MIMO system with 256 QAM.

Notations: Uppercase and lowercase boldface letters are used for matrices and vectors, respectively. The superscripts $(\cdot)^T$ and $(\cdot)^H$ denote the transpose and the Hermitage of a matrix, respectively. $|a|$ denotes the absolute value of a scalar a, or the cardinality of a if a is a set. $\|\cdot\|$ and $\lceil\cdot\rfloor$ represent the 2-norm of a vector and the rounding operation, respectively. $\mathbf{I}_N$ denotes the $N \times N$ identity matrix, and $\mathbf{0}_{M\times N}$ denotes an $M \times N$ matrix of all zeros.

2 Preliminaries

In the following subsections, we briefly explain the MIMO system model and introduce the lattice-reduced MIMO system model, whereby the channel matrix is transformed so that it has a favorable characteristic for MIMO detection. Moreover, we introduce the FSD—and the LR-aided FSD—which achieves near-optimal performance with low complexity.

2.1 MIMO system model

Consider a flat fading MIMO system with N_T transmit and N_R receive antennas, where $N_T \le N_R$. When $\mathbf{s} = [s_1, s_2, \ldots, s_{N_T}]^T$ denotes the transmitted symbol vector. The $N_R \times 1$ received symbol vector at one sample time can be expressed as follows:

$$\mathbf{y} = \mathbf{H}\mathbf{s} + \mathbf{n}, \tag{1}$$

where $\mathbf{n}$ denotes the $N_R \times 1$ additive white Gaussian noise (AWGN) vector with zero mean, the covariance matrix $E[\mathbf{n}\mathbf{n}^H] = \sigma_n^2\, \mathbf{I_{N_R}}$, and $\mathbf{H}$ represents an $N_R \times N_T$ channel matrix whose elements are independent and identically distributed (i.i.d.) complex Gaussian coefficients with zero mean and unit variance. We assume that the total power of every antenna is normalized to one, i.e., $E[\mathbf{s}^H\mathbf{s}] = 1$. We further assume that the channel matrix $\mathbf{H}$ varies at each sample time and is known by the receiver. Here, $\hat{\mathbf{s}}_{\mathrm{ML}}$, the MLD solution for (1), is given by

$$\hat{\mathbf{s}}_{\mathrm{ML}} = \underset{\mathbf{s}\in\Omega^{N_T}}{\arg} \min \|\mathbf{y} - \mathbf{H}\mathbf{s}\|^2, \tag{2}$$

where Ω denotes the constellation points. Whereas this MLD is optimal, its search space is proportional to $|\Omega|^{N_T}$. This exponential complexity renders the MLD infeasible for practical systems.

On the other hand, the zero-forcing (ZF) detector is the simplest linear detector, whose complexity is far lower than that of the MLD. The ZF detection can be formulated as follows:

$$\tilde{\mathbf{s}}_{\mathrm{ZF}} = \mathbf{H}^{\dagger}\mathbf{y} = \mathbf{s} + \mathbf{H}^{\dagger}\mathbf{n} = \mathbf{s} + \tilde{\mathbf{n}}, \tag{3}$$

$$\hat{\mathbf{s}}_{\mathrm{ZF}} = \mathcal{Q}(\tilde{\mathbf{s}}_{\mathrm{ZF}}) = \underset{\mathbf{s}\in\Omega^{N_T}}{\arg} \min |\tilde{\mathbf{s}}_{\mathrm{ZF}} - \mathbf{s}|, \tag{4}$$

where $\mathcal{Q}(\cdot)$ denotes the slicing (quantisation to a constellation point) operation, $\tilde{\mathbf{n}} := \mathbf{H}^{\dagger}\mathbf{n}$ denotes the noise amplified after linear equalisation, and $\mathbf{H}^{\dagger}$ is the Moore–Penrose pseudo-inverse of the channel matrix, which can be written as follows:

$$\mathbf{H}^{\dagger} = (\mathbf{H}^H\mathbf{H})^{-1}\mathbf{H}^H. \tag{5}$$

However, the noise amplification in (3) is the major cause of the degraded BER performance in linear detectors.

2.2 Lattice-reduced MIMO system model

To employ the lattice-reduced MIMO system model, the received signal is first scaled and shifted to map the received symbol to the consecutive complex integer lattice as follows:

$$\mathbf{x} = \frac{1}{\alpha}\mathbf{s} + \mathbf{1}_c, \tag{6}$$

where $\mathbf{1}_c = [1+j, \ldots, 1+j]^T$, α is the minimum distance between quadrature-amplitude-modulation (QAM) constellation points. The scaled and shifted received symbol vector can now be written as follows:

$$\dot{\mathbf{y}} \triangleq \frac{1}{\alpha}\mathbf{y} + \mathbf{H}\mathbf{1}_c = \mathbf{H}\left(\frac{1}{\alpha}\mathbf{s} + \mathbf{1}_c\right) + \frac{1}{\alpha}\mathbf{n} = \mathbf{H}\mathbf{x} + \dot{\mathbf{n}}, \tag{7}$$

where $\dot{\mathbf{n}} = \frac{1}{\alpha}\mathbf{n}$.

Let $\tilde{\mathbf{H}} = \mathbf{H}\mathbf{T}$ be the lattice-reduced channel matrix, where $\tilde{\mathbf{H}}$ spans the same lattice as $\mathbf{H}$ and $\mathbf{T}$ is a complex integer unimodular matrix. The lattice-reduced channel matrix $\tilde{\mathbf{H}}$ can be obtained from the complex LLL (CLLL) algorithm, which is summarised in Table 1.

Table 1 CLLL algorithm [16]

Input: $\mathbf{H}$

Output: $\tilde{\mathbf{Q}}, \tilde{\mathbf{R}}, \mathbf{T}$

Initialise: $[\mathbf{Q}, \mathbf{R}] = \mathrm{QRD}(\mathbf{H})$,

$\tilde{\mathbf{Q}} = \mathbf{Q}, \tilde{\mathbf{R}} = \mathbf{R}, \mathbf{T} = \mathbf{I}_{N_T}, k = 2$

1 : while $k \leq N_T$

2 : for $n = k-1 : -1 : 1$

3 : $\mu = \lceil \tilde{\mathbf{R}}(n,k)/\tilde{\mathbf{R}}(n.n) \rfloor$

4 : if $\mu \neq 0$

5 : $\tilde{\mathbf{R}}(1:n,k) = \tilde{\mathbf{R}}(1:n,k) - \mu\tilde{\mathbf{R}}(1:n,n)$

6 : $\mathbf{T}(:,k) = \mathbf{T}(:,k) - \mu\mathbf{T}(:,n)$

7 : end

8 : end

9 : if $\delta\,\tilde{\mathbf{R}}(k-1,k-1)^2 > \tilde{\mathbf{R}}(k,k)^2 + \tilde{\mathbf{R}}(k-1,k)^2$

10 : Swap columns $k-1$ and k in $\tilde{\mathbf{R}}$ and $\mathbf{T}$

11 : $\Theta = \begin{bmatrix} a^* & b \\ -b & a \end{bmatrix}$ with $a = \frac{\tilde{\mathbf{R}}(k-1,k-1)}{\|\tilde{\mathbf{R}}(k-1:k,k-1)\|}$, $b = \frac{\tilde{\mathbf{R}}(k-1,k-1)}{\|\tilde{\mathbf{R}}(k-1:k,k-1)\|}$

12 : $\tilde{\mathbf{R}}(k-1:k, k-1:N_T) = \Theta\tilde{\mathbf{R}}(k-1:k, k-1:N_T)$

13 : $\tilde{\mathbf{Q}}(:, k-1:k) = \tilde{\mathbf{Q}}(:, k-1:k)\Theta^H$

14 : $k = \max(k-1, 2)$

15 : else

16 : $k = k+1$

17 : end

18 : end

Line 2 − 8	: size reduction
Line 9	: Lovász condition
Line 10 − 13	: column swapping

If $\mathbf{z} = \mathbf{T}^{-1}\mathbf{x}$, the lattice-reduced system model can be represented as follows:

$$\dot{\mathbf{y}} = \mathbf{H}\mathbf{T}\mathbf{T}^{-1}\mathbf{x} + \dot{\mathbf{n}} = \tilde{\mathbf{H}}\mathbf{z} + \dot{\mathbf{n}}. \tag{8}$$

Then, the LR-aided ZF detector can be formulated as follows:

$$\mathbf{z}_{\text{LR-ZF}} = \tilde{\mathbf{H}}^{\dagger}\dot{\mathbf{y}} = \mathbf{z} + \tilde{\mathbf{H}}^{\dagger}\dot{\mathbf{n}} = \mathbf{z} + \mathbf{w}, \tag{9}$$

$$\hat{\mathbf{s}}_{\text{LR-ZF}} = \alpha\left(\mathbf{T}\lceil \mathbf{z}_{\text{LR-ZF}} \rfloor - \mathbf{1}_c\right). \tag{10}$$

Note that $\mathbf{w} := \tilde{\mathbf{H}}^{\dagger}\dot{\mathbf{n}}$ in (9) is the noise amplified by the lattice-reduced channel matrix $\tilde{\mathbf{H}}^{\dagger}$. With the aid of the near-orthogonal nature of the lattice-reduced matrix, the noise amplification in (9) is much less than (3) so that the BER performance of LR-aided linear detectors has the same diversity order as the MLD.

2.3 FSD

Through the QRD on the channel matrix $\mathbf{H}$, $\mathbf{H}$ can be decomposed as $\mathbf{H} = \mathbf{Q}\mathbf{R}$, where $\mathbf{Q}$ is an $N_R \times N_T$ unitary matrix, and $\mathbf{R}$ is an $N_T \times N_T$ upper-triangular matrix. By multiplying both sides of (1) by $\mathbf{Q}^H$, the system model can be rewritten as follows:

$$\mathbf{q} = \mathbf{R}\mathbf{s} + \mathbf{v}, \tag{11}$$

where $\mathbf{q} = \mathbf{Q}^H\mathbf{y}$ and $\mathbf{v} = \mathbf{Q}^H\mathbf{n}$. Figure 1 shows that the FSD performs constrained tree searching on (11), which consists of the full expansion (FE) and single expansion (SE) stages. For the first N_p levels, FE is performed, where all possible $|\Omega|$ branches are expanded. Then, for the remaining $N_T - N_p$ levels, SE is performed, where only one branch is expanded on each node in the manner of SIC. In other words, the FSD solution is given by

$$\hat{\mathbf{s}}_{\text{FSD}} = \underset{\mathbf{s} \in \mathcal{L}}{\arg\min} \|\mathbf{q} - \mathbf{R}\mathbf{s}\|^2, \tag{12}$$

where $\mathcal{L}$ is the candidate list, which is generated as follows:

$$\mathcal{L} = \left[\tilde{\mathbf{s}}_1, \tilde{\mathbf{s}}_2, \cdots, \tilde{\mathbf{s}}_{|\Omega|^{N_p}}\right], \tag{13}$$

where $\tilde{\mathbf{s}}_l = [\tilde{s}_{l,1}, \cdots, \tilde{s}_{l,N_T}]^T$ and

$$\tilde{s}_{l,i} = \left\{ \begin{array}{lr} \in \Omega\,, \quad i = N_T, \cdots, N_T - N_p + 1 & \\ \mathcal{Q}\left(\left(q_i - \sum_{j=i+1}^{N_T} r_{i,j}\tilde{s}_{l,j}\right)/r_{i,i}\right), & \text{else,} \end{array} \right\} \tag{14}$$

where q_i and $r_{i,j}$ are the ith element in $\mathbf{q}$ and the (i,j)th element in $\mathbf{R}$, respectively. In order to achieve optimal performance, the channel matrix should be ordered prior to tree searching so that the signals with maximum and minimum post-processing noise amplifications are detected at the FE and SE stages, respectively [3]. Throughout this paper, to simplify the notation, we consider the channel matrices and transmit signals as corresponding variables with permutations.

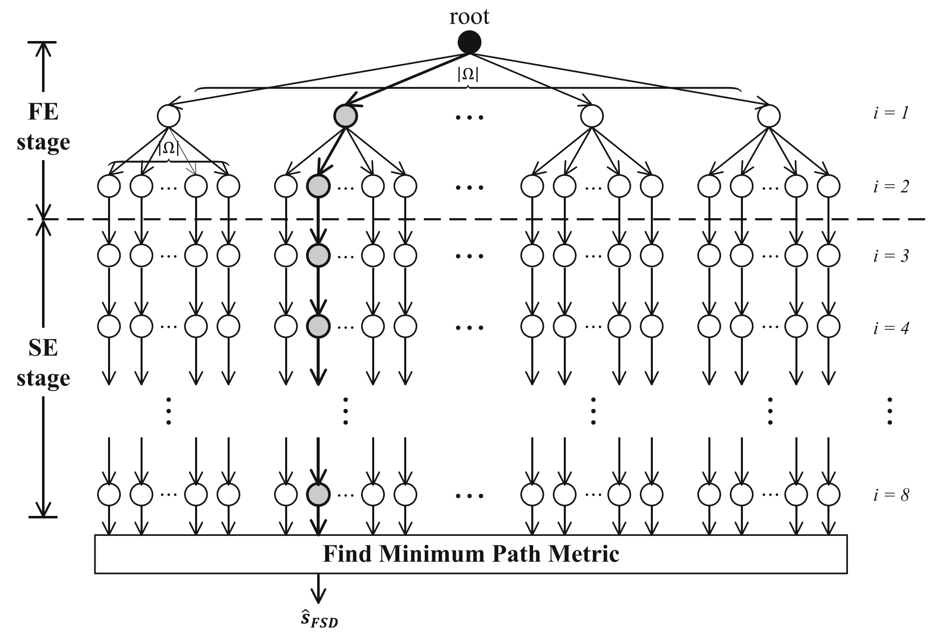

Fig. 1 Tree structure of the FSD on an 8 × 8 MIMO system with |Ω|-QAM and $N_p = 2$. The gray-colored tree node contains the FSD solution

2.4 LR-aided FSD [15]

In order to reduce the complexity, the LR-aided FSD algorithm lowers the number of tree levels in the FE stage, in order to reduce the parent nodes generated at the FE stage. Nevertheless, the proposed algorithm maintains near-optimal BER performance by adopting LR-aided SIC at the SE stage. However, the application of the LR algorithm to the FSD is not straightforward. The bases of the channel matrix are modified in the lattice-reduced system model so that the child nodes cannot be expanded [10]. Hence, the LR-aided FSD generates the candidate signal in the FE stage, and cancel the FE signals in the original constellation domain before transforming the system model into a lattice-reduced one.

In other words, the FE candidate signals are cancelled and nulled as follows:

$$\mathbf{y}'_{(k)} = \mathbf{y} - \sum_{l=N_T-N_p+1}^{N_T} \mathbf{h}_l \hat{s}_{l(k)}, \tag{15}$$

where $\mathbf{y}'_{(k)}$ denotes the $N_R \times 1$ received signal in the revised system model, $\mathbf{h}_l$ is the lth column vector of the channel matrix $\mathbf{H}$, and $\hat{s}_{l(k)}$ is the kth FE candidate signal transmitted from the lth transmit antenna. Then, the system model is transformed to a nulled system model as follows:

$$\mathbf{y}'_{(k)} \triangleq \mathbf{H}'\mathbf{s}'_{(k)} + \mathbf{n}, \tag{16}$$

where $\mathbf{H}'$ and $\mathbf{s}'_{(k)}$ respectively denote the $N_R \times \left(N_T - N_p\right)$ channel matrix and the $\left(N_T - N_p\right) \times 1$ transmitted signal whose lth $\left(l = N_T - N_p + 1, \cdots, N_T\right)$ column vectors and elements are nulled. Then, LR-aided SIC is performed on (16) to complete the candidate list, and the detection is completed by the ML test, where the symbol vector with the minimum Euclidean distance (ED) is detected as the solution.

3 Proposed algorithm

3.1 Motivation

Motivated by the previous analysis in [25], we conducted a hypothetical experiment to determine whether it is fundamentally possible to apply the ET scheme to LR-aided detectors other than the LR-aided SIC detector, as illustrated in Fig. 2. First, the LR-aided FSD solution $\hat{\mathbf{s}}_{\text{LR-FSD}}$ was obtained using the channel matrix that passed the basis-reduction process with the original CLLL. Then, at the end of each CLLL iteration, the temporary LR-aided FSD solution $\hat{\mathbf{s}}_{\text{tmp}}$ was obtained with the intermediate lattice-reduced channel condition. We compared $\hat{\mathbf{s}}_{\text{LR-FSD}}$ and $\hat{\mathbf{s}}_{\text{tmp}}$ at each CLLL iteration, and terminated the reduction process when the two solutions were the same—referred to as the ideal ET.

We performed this simulation on an 8×8 MIMO system with 256-QAM and $N_p = 1$. As shown in Fig. 3, a considerable portion of the CLLL process is unnecessary in the context of MIMO detection with the LR-aided FSD, especially at high E_b/N_o values. Hence, it can be concluded that it is indeed fundamentally possible to employ the ET in the LR-aided FSD.

Given this inference, ILR can be rendered a practical ET scheme by adopting the RA in [26], which is formulated as follows:

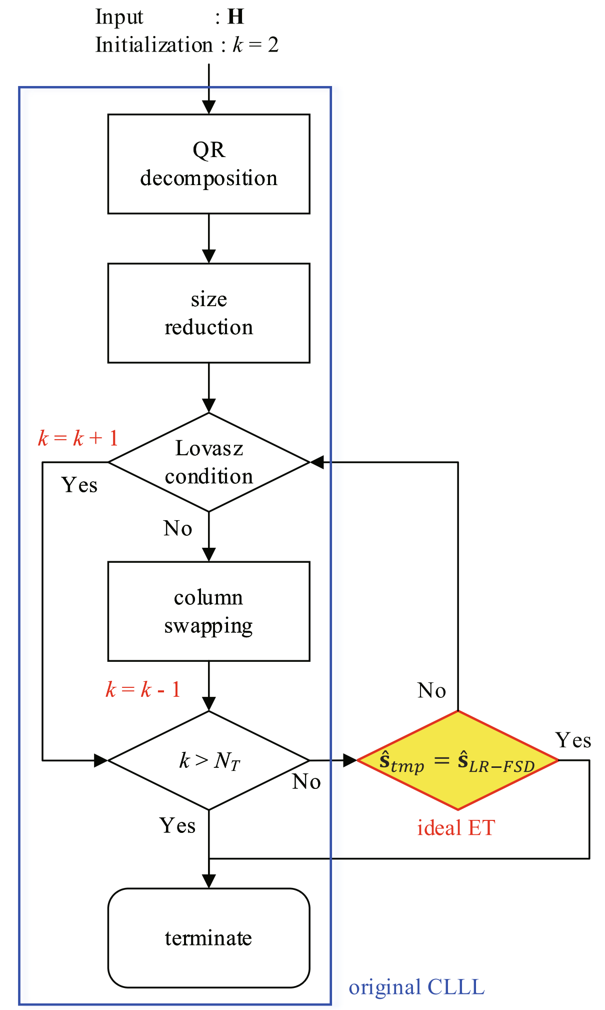

Fig. 2 Flow chart for CLLL with ideal ET. Here, $\hat{\mathbf{s}}_{\text{LR-FSD}}$ is the LR-aided FSD solution with the original CLLL, and $\hat{\mathbf{s}}_{\text{tmp}}$ is the LR-aided FSD solution obtained at each iteration

$$\|\mathbf{y} - \mathbf{H}\hat{\mathbf{s}}_{\text{tmp}}\|^2 \leq A\sigma_n^2, \tag{17}$$

where A is the positive parameter that determines the tradeoff between performance and computational complexity. However, there is a critical issue in the application of the ET to the LR-aided FSD. Whereas ILR obtained the practical ET criterion with RA by performing partial SIC detection during the intermediate LR process, all parent nodes should be considered as the candidate signal in the LR-aided FSD, making the overhead incurred by the partial detection too large. A novel way of handling this obstacle is proposed in the next subsection.

3.2 CLLL with ET for the LR-aided FSD

A problem arises when applying conventional ILR directly to the LR-aided FSD [15]: all the parent nodes in the FE stage should be considered for partial detection, making the overhead incurred by the partial detection too large. In order to solve this problem, the proposed algorithm exchanges the column vectors of the channel matrix corresponding to the FE stage and SE stage. LR is performed on column vectors during the SE stage exclusively, and not during the FE stage. In this way, as the LR-aided FSD performs LR-aided detection during the SE stage, the column vectors that actually involve LR-aided detection are lattice-reduced. Furthermore, because the signals of the SE stage are switched to the upper level of the tree structure, partial detection with SIC can be performed on the corresponding signals.

Let us explain in more detail the proposed algorithm with in a 4×4 MIMO system. The system model in (1) can be written in a 4×4 MIMO system as

$$\mathbf{y} = \mathbf{H}\mathbf{s} + \mathbf{n} = \mathbf{h}_1 s_1 + \mathbf{h}_2 s_2 + \mathbf{h}_3 s_3 + \mathbf{h}_4 s_4 + \mathbf{n}. \tag{18}$$

Then, the LR-aided FSD with $N_p = 1$ transforms the system model to a nulled system model as

$$\mathbf{y}'_{(k)} \triangleq \mathbf{H}'\mathbf{s}' + \mathbf{n} \triangleq \mathbf{h}_1 s_1 + \mathbf{h}_2 s_2 + \mathbf{h}_3 s_3 + \mathbf{n}. \tag{19}$$

In order to perform the LR-aided SIC detection on the SE stage, (19) is transformed to a lattice-reduced system model as

$$\mathbf{y}'_{(k)} \triangleq \mathbf{H}'\mathbf{s}' + \mathbf{n} = \mathbf{H}'\mathbf{T}'\mathbf{T}'^{-1}\mathbf{s}' + \mathbf{n} \triangleq \tilde{\mathbf{H}}'\mathbf{z}' + \mathbf{n}, \tag{20}$$

where $\tilde{\mathbf{H}}' \triangleq \mathbf{H}'\mathbf{T}'$ and $\mathbf{z}' \triangleq \mathbf{T}'^{-1}\mathbf{s}'$. Also, $\mathbf{T}'$ is the transformation matrix to assure the lattice-reduced characteristics of $\mathbf{H}'$, which is obtained by performing the LLL to $\mathbf{H}'$. Here, $\mathbf{T}'$ needs to assure the lattice-reduced characteristics between the column vectors $\{\mathbf{h}_1, \mathbf{h}_2, \mathbf{h}_3\}$, not $\mathbf{h}_4$. Hence, the proposed algorithm obtains $\mathbf{T}'$ based on a different system model as

$$\mathbf{y} = \bar{\mathbf{H}}\bar{\mathbf{s}} + \mathbf{n}, \quad \left(\bar{\mathbf{H}} = [\mathbf{h}_4, \mathbf{H}'], \ \bar{\mathbf{s}} = [s_4, \mathbf{s}']\right) \tag{21}$$

where, the channel column vector and the transmit signal corresponding to the FE signal are moved to the front column and row, respectively. Then, whereas the conventional LLL starts from the first column, the proposed algorithm skips the first column and performs the LLL processing only on $\mathbf{H}'$. In other words, the initial value of the column index k is changed from 2 to 3. The output of the proposed algorithm is a 4×4 transformation matrix $\bar{\mathbf{T}}$ whose right-lower submatrix is the same as $\mathbf{T}'$, which means that $\bar{\mathbf{T}} = \begin{bmatrix} 1 & \mathbf{0}_{1\times 3} \\ \mathbf{0}_{3\times 1} & \mathbf{T}' \end{bmatrix}$.

Here, we perform the partial SIC during the LLL processing to obtain the signal $\mathbf{s}'$ which is used to compute the RA in (17). There might exist some false ETs, because the RA is computed with a signal which is obtained by not the original FSD but the SIC on the SE stage. This leads to a trade-off between the BER performance and the computational complexity as a function of the parameter A in

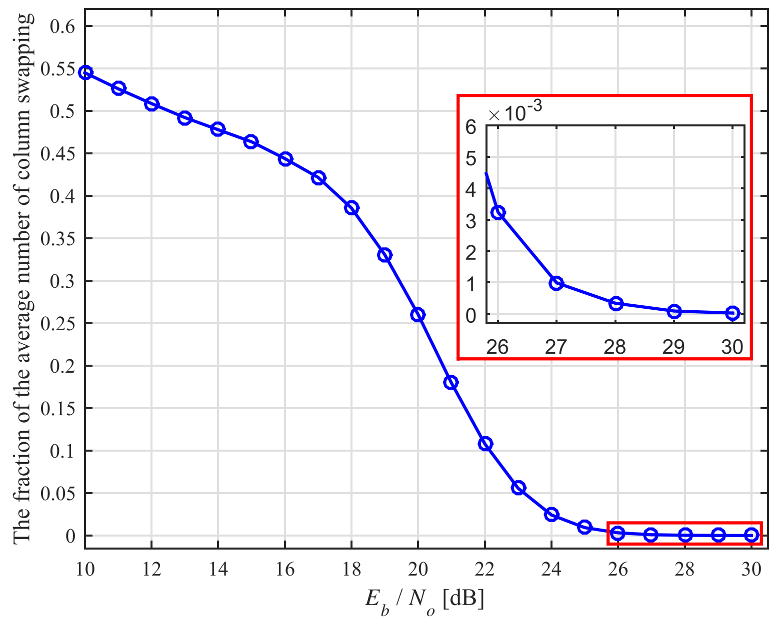

Fig. 3 Fraction of the average number of column swaps, compared to the original CLLL. The simulation was conducted using the LR-aided FSD on an 8×8 MIMO system with 256-QAM and $N_p = 1$

(17). However, the proposed algorithm reduces the complexity considerably with little performance degradation, which is shown in the next Section.

The proposed algorithm is summarised in Table 2 and has the following main features.

3.2.1 Input channel matrix conversion (line 1 in Table 2)

First, the column vectors of $\mathbf{H}$ corresponding to the FE stage and SE stage are exchanged, resulting in a converted channel matrix $\bar{\mathbf{H}}$. In this way, signals corresponding to the SE stage are displaced to the upper level in the tree structure so that partial SIC detection can be applied to the corresponding signals without considering the parent nodes during the FE stage.

3.2.2 Modification of the index for LR processing

The LR-aided FSD priorly eliminates FE signals and performs LR-aided SIC detection during the SE stage. This means that column vectors corresponding to the SE stage are those that actually require the basis-reduction process. Hence, as detailed in the initialization step and line 21 in Table 2, the column search index for LR processing, k, is modified from $[2, \cdots, N_T]$ to $\left[2 + N_p, \cdots, N_T\right]$.

3.2.3 ET check (lines 4–17 in Table 2)

Prior to each LR iteration, an ET check is performed by adopting the RA criterion, which is computed by the symbol partially detected with the intermediate lattice-reduced channel. If the detected symbol is within the predetermined boundary, LR processing is terminated. Note that this operation is performed only when column swapping occurs so that the channel condition is modified. Furthermore, the symbol index where partial detection is performed is determined according to the column-swapping index, as shown in line 23 in Table 2.

3.2.4 Modified QRD (line 2 in Table 2)

The LR-aided FSD uses the nulled channel matrix, $\mathbf{H}'$ in (16), which consists of the column vectors of the channel matrix corresponding to the SE stage, as the input of the CLLL process. Meanwhile, the proposed algorithm uses the full channel matrix $\mathbf{H}$ after converting to $\bar{\mathbf{H}}$. Let $\mathbf{H}' = \mathbf{Q}'\mathbf{R}'$ and $\bar{\mathbf{H}} = \bar{\mathbf{Q}}\bar{\mathbf{R}}$, which are the results of the QRD. Then, the output matrices $(\mathbf{Q}', \mathbf{R}')$ and $(\bar{\mathbf{Q}}, \bar{\mathbf{R}})$ differ from each other. This means that the proposed algorithm performs LR in an undesired manner, as LR processing is dependent on the QRD result.

To overcome this problem, we modified the QRD algorithm in the proposed algorithm, which is based on the QRD with the Gram–Schmidt (GS) process. The proposed modification to the QRD algorithm is summarised in Table 3. Unlike the original QRD, the modified QRD performs the GS process for the column vectors of the channel matrix corresponding to the SE stage, generating an orthonormalized basis. This orthonormal matrix results in a unitary matrix $\bar{\mathbf{Q}}$, which is equivalent to $\mathbf{Q}'$. Then, the $\bar{\mathbf{Q}}^H$ is multiplied by $\bar{\mathbf{H}}$, resulting in a partially upper-triangular matrix $\bar{\mathbf{R}}$, whose right-side column vectors are identical to $\mathbf{R}'$—i.e. $\bar{\mathbf{R}}\left(:, N_p + 1 : N_T\right) = \mathbf{R}'$.

Table 2 Proposed CLLL algorithm with ET for the LR-aided FSD

Input: $\mathbf{H}$, $\mathbf{y}$
Output: $\bar{\mathbf{T}}$
Initialise: $k = 2 + N_p$, $update = 1$, $l = N_T - N_p$
$\bar{\mathbf{T}} = \mathbf{I}_{N_T - N_p}$, $\mathbf{p} = \mathbf{0}_{(N_T - N_p)\times 1}$

$\bar{\mathbf{H}} = \left[\mathbf{H}\left(:, N_T - N_p + 1 : N_T\right), \mathbf{H}\left(:, 1 : N_T - N_p\right)\right]$
$\left[\bar{\mathbf{Q}}, \bar{\mathbf{R}}\right] = \text{Modified\_QRD}\left(\bar{\mathbf{H}}, N_p\right)$, $\tilde{\mathbf{Q}} = \bar{\mathbf{Q}}$, $\tilde{\mathbf{R}} = \bar{\mathbf{R}}$
while($k \le N_T$)
  if(*update*)
    $\mathbf{q} = \mathbf{Q}^H \mathbf{y}$
    for $n = l : -1 : 1 + N_p$
      if $n < (N_T - N_p)$
        $\mathbf{p}(n) = \left\lceil \frac{\mathbf{q}(n) - \tilde{\mathbf{R}}(n, n+N_p+1 : N_T)}{\tilde{\mathbf{R}}(n, n+N_p)} \right\rfloor$
      else
        $\mathbf{p}(n) = \left\lceil \frac{\mathbf{q}(n)}{\tilde{\mathbf{R}}(n, n+N_p)} \right\rfloor$
      end
    end
    $ED = \text{sum}\left(\|\mathbf{q} - \tilde{\mathbf{R}}(:, 1 + N_p : N_T)\mathbf{p}\|^2\right)$
    if$\left(ED < A\sigma_n^2\right)$
      break
    end
  end
  Size_Reduction (for $n = k - 1 : -1 : N_p$)
  if $\delta\, \tilde{\mathbf{R}}\left(k - 1 - N_p, k - 1\right)^2 > \tilde{\mathbf{R}}\left(k - N_p, k\right)^2 + \tilde{\mathbf{R}}\left(k - 1 - N_p, k\right)^2$
    Column_Swapping (of $k - 1$ and k)
    $k = \max\left(k - 1, 2 + N_p\right)$
    update = 1
    $l = k$
  else
    $k = k + 1$
    update = 0
  end
end

Modified_QRD	: in Table 3
Size_Reduction	: Line 2–8 in Table 1
Column_Swapping	: Line 10–13 in Table 1

Table 3 Modified QRD algorithm

Input: $\bar{\mathbf{H}}$, N_p
Output: $\bar{\mathbf{Q}}$, $\bar{\mathbf{R}}$
Initialise: $\mathbf{B} = \mathbf{0}_{N_R \times (N_T - N_p)}$, $\bar{\mathbf{Q}} = \mathbf{0}_{N_R \times (N_T - N_p)}$

for $k = 1 : N_T - N_p$
  $\mathbf{B}(:, k) = \bar{\mathbf{H}}\left(:, k + N_p\right)$
  for $l = 1 : k - 1$
    $\mathbf{B}(:, k) - \frac{\mathbf{B}(:, l)^H \bar{\mathbf{H}}(:, k+N_p)}{\|\mathbf{B}(:, l)\|^2}$
  end
  $\bar{\mathbf{Q}}(:, k) = \frac{\mathbf{B}(:, k)}{\|\mathbf{B}(:, k)\|}$
end
$\bar{\mathbf{R}} = \bar{\mathbf{Q}}^H \bar{\mathbf{H}}$

Although the leftmost column vector of $\bar{\mathbf{R}}$ affects the partial SIC detection in the ET check as the interference, each element in the vector is statistically smaller than the diagonal terms of $\mathbf{R}'$. This is because the power of the leftmost terms of $\bar{\mathbf{R}}$ are distributed normally, whereas the power of $\mathbf{R}'$ are converged to the diagonal terms due to the FSD ordering. Table 4 presents the average power of the diagonal terms of $\mathbf{R}'$, the leftmost terms of $\bar{\mathbf{R}}$, and the fraction of the leftmost terms normalized by the diagonal terms on each tree level. Consequently, the interference of the leftmost column vector is nominal.

4 Simulation results

In this section, the BER performance and the computational complexity of the conventional CLLL is compared to that of the proposed CLLL with ET for LR-aided FSD through computer simulations. The simulation was conducted on an uncoded 8×8 MIMO system with 256-QAM, with $N_p = 1$ for LR-aided FSD. Here, E_b denotes the average energy per information bit arriving at the receiver. Thus, the signal-to-noise-ratio (SNR) is given by $E_b/N_o = N_R/\left(\log_2(|\Omega|)\sigma_n^2\right)$.

Figure 4 shows the uncoded BER performance of the SD, FSD, and LR-aided FSD with different LR algorithms, as a function of E_b/N_o. Because the time consumption of

Table 4 The average power of the diagonal terms of $\mathbf{R}'$, the leftmost terms of $\bar{\mathbf{R}}$, and the fraction of the leftmost terms normalized by the diagonal terms on each tree level. The channel condition is given by the Rayleigh fading channel ordered by the FSD channel ordering

Tree level	Diagonal terms	Leftmost terms	Fraction
1	4.1858	0.0879	0.0210
2	3.7763	0.1615	0.0428
3	4.0852	0.2603	0.0367
4	4.5849	0.3727	0.0813
5	5.0649	0.5306	0.1048
6	5.6178	0.7442	0.1325
7	6.3230	1.4036	0.2220
Average	4.8054	0.5087	0.1059

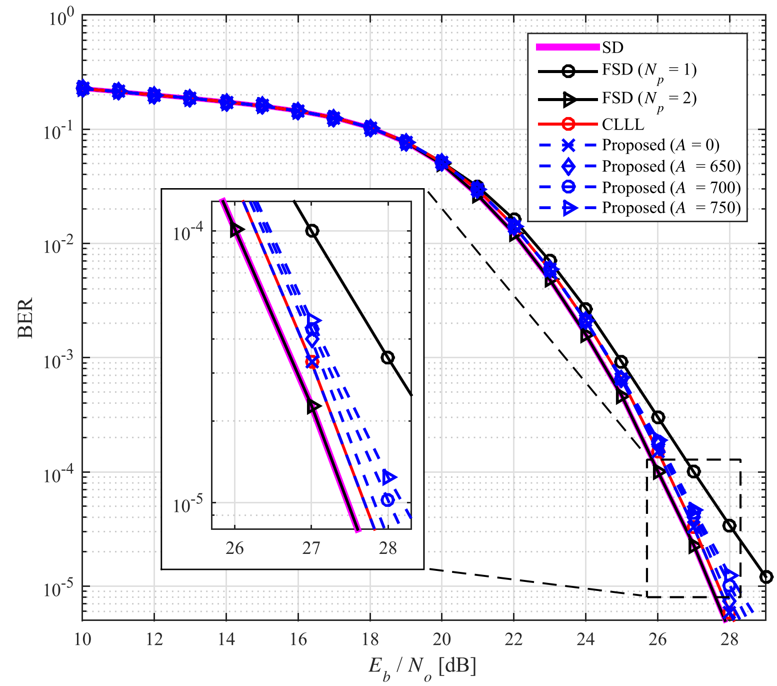

Fig. 4 Comparison of the uncoded BER performance of MIMO detectors. The simulation was conducted on an uncoded 8 × 8 MIMO system with 256-QAM, with $N_p = 1$ for the LR-aided FSD

the optimal ML simulation is too high, the optimal performance was obtained by performing the simulation with the SD. In order to achieve near-optimal performance, the FSD must satisfy $N_p \geq \sqrt{N_T} - 1$, if $N_T = N_R$ holds. This means that $N_P \geq 2$ must hold when $N_T = N_R = 8$ [27]. Therefore, there was considerable performance degradation for the FSD with $N_p = 1$, whereas the FSD with $N_p = 2$ achieved near-optimal performance.

By contrast, the LR-aided FSD with CLLL achieved near-optimal performance despite an insufficient number

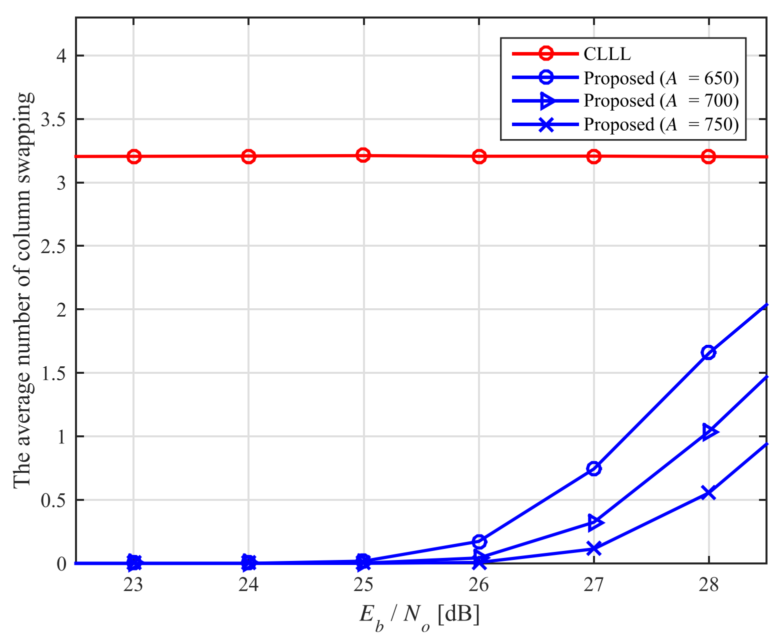

Fig. 5 Average number of column swaps in the LR algorithms as a function of E_b/N_o

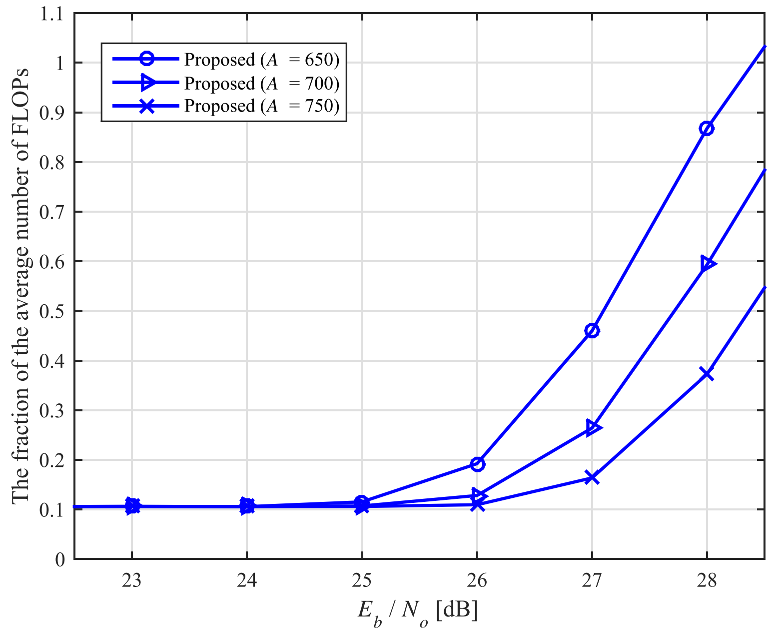

Fig. 6 Fraction of the average number of FLOPs from the proposed LR algorithm normalized by the conventional CLLL as a function of E_b/N_o

of FE stage. Moreover, when the proposed LR algorithm was applied, the performance degradation with the LR-aided FSD was less than 0.5 dB for $A \leq 700$ at a BER of 10^{-5}. Note that the performance of the conventional CLLL and the proposed algorithm for $A = 0$ was the same because no ET occurred. Meanwhile, Fig. 5 shows the reduction in the average number of column swaps in the LR algorithms, which is the celebrated indicator of the computational complexity of the LR algorithm. Contrary to the result with the ideal ET which is shown in Fig. 3, the average number of column swaps increases for higher SNR. This is because the threshold of the RA gets tighter as the noise variance decreases. As the performance degradation is more sensitive to the channel

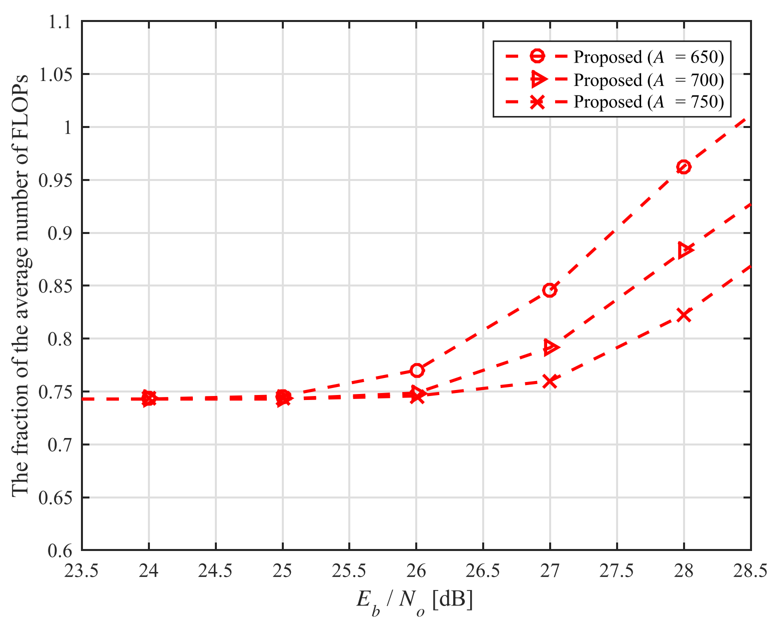

Fig. 7 Fraction of the average number of FLOPs from the LR-aided FSD with the proposed LR algorithm normalized by the one with the conventional CLLL as a function of E_b/N_o

condition for higher SNR, it is inevitable to get the threshold tighter. Nevertheless, the average number of column swaps in the proposed algorithm with $A = 700$ was reduced to approximately 30 % of that of the CLLL at $E_b/N_o \approx 28$ dB where the BER is approximately 10^{-5}.

For a more generalized comparison, the computational complexity was analysed in terms of the number of floating point operations (FLOPs), which we obtained according to the following rules [28]:

- The multiplication of $l \times m$ and $m \times n$ real (complex) matrices requires $2\,lmn$ ($8\,lmn$) FLOPs.
- The Moore–Penrose pseudo-inverse of an $m \times n$ real matrix requires $2m^3 - 2m^2 + m + 16mn$ FLOPs.

Figure 6 illustrates the average number of FLOPs from the proposed LR algorithm normalized by the conventional CLLL. Although there was overhead owing to the ET check, the complexity of the proposed LR algorithm with $A = 700$ was reduced by approximately 40 % at $E_b/N_o = 28$ dB where the BER is approximately 10^{-5}.

In Fig. 7, the average number of FLOPs from the LR-aided FSD with the proposed LR algorithm normalized by the one with the conventional CLLL is illustrated. As the complexity of the FSD is not negligible, the reduction rate of the FLOPs is decreased, compared to the results in Fig. 6. However, there still exists the decrease in the computational complexity which is approximately 18 % at $E_b/N_o = 28$ dB where the BER is approximately 10^{-5}. Note that this reduction rate can be increased, if the proposed algorithm adopts the low-complexity FSD algorithms such as simplified FSD [29] or FSD with pruning [30].

5 Conclusions

In this paper, we proposed a low-complexity LR algorithm with ET for detectors with tree searching. Whereas the ILR [25] is limited to LR-aided SIC detectors, the proposed algorithm is an extension of the conventional approach to LR for detectors with tree searching. We performed an additional hypothetical analysis and several novel modifications to the conventional algorithm in order to overcome its limitations.

We verified the performance of the proposed algorithm with a computer simulation, demonstrating that the average number of column swaps was reduced, with negligible BER performance degradation. Furthermore, for a fair comparison, the computational complexity was analysed in terms of the number of FLOPs, indicating a significant reduction in computational complexity.

Acknowledgments
This work was supported by the National Research Foundation of Korea(NRF) grant funded by the Korea government(MSIP) (No. NRF-2015R1A2A2A0100 4883).

Competing interests
The authors declare that they have no competing interests.

Received: 22 May 2016 Accepted: 14 October 2016
Published online: 18 January 2017

References

1. E Viterbo, J Boutros, A univeral lattice code decoder for fading channels. IEEE Trans. Inform. Theory. **45**(5), 1639–1642 (1999)
2. MO Damen, HE Gamal, G Caire, On maximum-likelihood detection and the search for the lattice point. IEEE Trans. Inform. Theory. **49**(10), 2389–2402 (2003)
3. L Barbero, J Thompson, Fixing the complexity of the sphere decoder for MIMO detection. IEEE Trans. Wirel. Commun. **7**(6), 2131–2142 (2008)
4. C Xiong, X Zhang, K Wu, D Yang, A simplified fixed-complexity sphere decoder for V-BLAST systems. IEEE Commun. Lett. **13**(8), 582–584 (2009)
5. KW Wong, CY Tsui, RK Cheng, WH Mow, A VLSI architecture of a K-Best lattice decoding algorithm for MIMO channels. IEEE Int. Symp. Circuits Syst. **3**, 273–276 (2002)
6. H Yao, HW Wornell, Lattice-reduction-aided detectors for MIMO communications systems. IEEE Global Telecommun. Conf. **1**, 424–428 (2002)
7. D Wübben, R Böhnke, V Kühn, KD Kammeyer, Near-maximum-likelihood detection of MIMO systems using MMSE-based lattice reduction. IEEE Int. Conf. Commun. **2**, 798–802 (2004)
8. M Taherzadeh, A Mobasher, AK Khandani, LLL reduction achieves the receive diversity in MIMO decoding. IEEE Trans. Inform. Theory. **53**(12), 4801–4805 (2007)
9. J Jaldén, P Elia, DMT optimality of LR-aided linear decoders for a general class of channels, lattice designs, system models. IEEE Trans. inform. Theory. **56**(10), 4765–4780 (2010)
10. M Shabany, P Gulak, The application of lattice-reduction to the K-best algorithm for near-optimal MIMO detection. IEEE Int. Symp. Circuits Syst, 316–319 (2008)
11. M Shabany, P Gulak, A 675 Mbps, 4×4 64-QAM K-best MIMO detector in 0.13 μm CMOS. IEEE Trans. Very Large Scale Integr. (VLSI) Syst. **20**(1), 135–147 (2012)
12. S Aubert, Y Nasser, F Nouvel, Lattice-reduction-aided minimum mean square error K-best detection for MIMO systems. IEEE Int. Conf. Comput. Netw. Commun. **2**, 798–802 (2004)
13. H Kim, J Park, H Lee, J Kim, Near-ML MIMO detection algorithm with LR-aided fixed-complexity tree searching. IEEE Commun. Lett. **18**(12), 2221–2224 (2014)
14. J Liu, S Xing, L Shen, Lattice-reduction-aided sphere decoding for MIMO detection achieving ML performance. IEEE Commun. Lett. **20**(1), 125–128 (2016)
15. H Kim, J Kim, Near-optimal MIMO detection algorithm with low and fixed complexity. IEEE Int. Symp. Consumer Electron, 1–2 (2015)
16. YH Gan, C Ling, WH Mow, Complex lattice reduction algorithm for low-complexity full-diversity MIMO detection. IEEE Trans. Signal Prcoess. **57**(7), 2701–2710 (2009)
17. AK Lenstra, HW Lenstra, L Lovász, Factoring polynomials with rational coefficients. Math. Ann. **261**, 515–534 (1982)
18. C Ling, N Howgrave-Graham, Effective LLL reduction for lattice decoding. IEEE Int. Symp. Inform. Theory, 196–200 (2007)
19. W Zhang, S Qiao, Y Wei, A diagonal lattice reduction algorithm for MIMO detection. IEEE Signal Process. Lett. **19**(5), 311–314 (2012)
20. K Zhao, S Du, Full-diversity approximated lattice reduction algorithm for low-complexity MIMO detction. IEEE Commun. Lett. **18**(6), 1079–1082 (2014)
21. H Vetter, V Ponnampalam, M Sandell, PA Hoeher, Fixed-complexity LLL algorithm. IEEE Trans. Signal Process. **57**(4), 1634–1637 (2009)
22. K Zhao, H Jiang, Y Li, S Du, Random selection LLL algorithm and its fixed complexity variant for MIMO detection. Int. Symp. Wirel. Personal Multimed. Commun, 1–5 (2011)
23. C Ling, WH Mow, N Howgrave-Graham, Reduced and fixed-complexity variants of the LLL algorithm for communications. IEEE Trans. Commun. **61**(3), 1040–1050 (2013)
24. Q Wen, Q Zhou, X Ma, An enhanced fixed-complexity LLL algorithm for MIMO detection. IEEE Global Telecommun. Conf. **1**, 3231–3236 (2014)

25. B Gestner, X Ma, DV Anderson, Incremental lattice reduction: motivation, theory, and practical implementation. IEEE Trans. Wirel. Commun. **11**(1), 188–198 (2012)
26. F Wang, Y Xiong, X Yang, Reliability assessment for MIMO detection and its applications. Int. J. Electron. Commun. **63**(8), 678–684 (2009)
27. J Jaldén, LG Barbero, B Ottersten, JS Thompson, Full-diversity detection in MIMO systems with a fixed-complexity sphere decoder. IEEE Int. Conf. Acoustics Speech Signal Process. **3**, 49–52 (2007)
28. GH Golub, CF Van Loan, *Matrix computations*. (The Johns Hopkins University Press, Baltimore, 2013)
29. C Xiong, X Zhang, K Wu, D Yang, A simplified fixed-complexity sphere decoder for V-BLAST Systems. IEEE Commun. Lett. **13**(8), 582–584 (2009)
30. S Lei, Q Tu, D Yang, J Chen, Probabilistic tree pruning for fixed-complexity sphere decoder in MIMO systems. IEEE Int. Conf. Wirel. Commun. Signal Process, 1–6 (2010)